Hindawi
Mathematical Problems in Engineering
Volume 2020, Article ID 3658146, 11 pages
https://doi.org/10.1155/2020/3658146

Research Article

An Improved Analytical Method for Vibration Analysis of Variable Section Beam

Jingjing Feng[1,2] **Zhengneng Chen,**[1,2] **Shuying Hao,**[1,2] **and Kunpeng Zhang**[1,2]

[1]*Tianjin Key Laboratory for Advanced Mechatronic System Design and Intelligent Control, School of Mechanical Engineering, Tianjin University of Technology, Tianjin 300384, China*
[2]*National Demonstration Center for Experimental Mechanical and Electrical Engineering Education, Tianjin University of Technology, Tianjin 300384, China*

Correspondence should be addressed to Jingjing Feng; jjfeng@tju.edu.cn and Kunpeng Zhang; kpzhang@email.tjut.edu.cn

Received 1 April 2020; Accepted 22 July 2020; Published 17 August 2020

Academic Editor: José A. Sanz-Herrera

The variable section structure could be the physical model of many vibration problems, and its analysis becomes more complicated either. It is very important to know how to obtain the exact solution of the modal function and the natural frequency effectively. In this paper, a general analytical method, based on segmentation view and iteration calculation, is proposed to obtain the modal function and natural frequency of the beam with an arbitrary variable section. In the calculation, the section function of the beam is considered as an arbitrary function directly, and then the result is obtained by the proposed method that could have high precision. In addition, the total amount of calculation caused by high-order Taylor expansion is reduced greatly by comparing with the original Adomian decomposition method (ADM). Several examples of the typical beam with different variable sections are calculated to show the excellent calculation accuracy and convergence of the proposed method. The correctness and effectiveness of the proposed method are verified also by comparing the results of the several kinds of the theoretical method, finite element simulation, and experimental method.

1. Introduction

The vibration energy harvesters often use the cantilever beam for the basic oscillator because of its simple structure, low rigidity, high energy density of bending vibration, and so on. The variable section structure shows some special performance, so it has excellent prospects in the field of the vibration piezoelectric energy harvester and attracts wide attention [1–4]. Ooi et al. [1] studied the energy harvester systems, which are composed of five cantilever beam models with different sections. Then, the strain of each part is analyzed, when external loads are applied to the free end of the cantilever beam. The results show that the piezoelectric property of the triangular beam is more effective. Adopting the theoretical and experimental method, Savarimuthu et al. [2] discussed the influence of the position of the piezoelectric plate on the piezoelectric efficiency which was generated by vibration of the beam with different sections under the same vibration conditions. Wang et al. [3] analyzed the influence of the beam width at the free end of the cantilever beam on natural frequency and piezoelectric efficiency through finite element simulation.

It is necessary to solve the modal function and natural frequency for studying the vibration characteristics of the beam [5–8]. For the uniform beam, section area and stiffness of the microsection in the discrete body model are constant and equal. For the variable section beam, the section area and stiffness are functions of the section position, which makes the constant coefficients of the differential equation in the traditional method to become a variable coefficient. As a result, it is impossible to apply directly the traditional method to analyze the modal function and natural frequency of those beams with variable section. In order to solve this problem and analyze its vibration characteristics, various analytical methods are proposed. Basing on the Galerkin method, Pielorz and Nadolski [9] developed a modal

analysis method for a thin beam with a variable section. Laura et al. [10] optimized the Rayleigh–Ritz method to obtain natural frequency of the beam with constant width and hyperbolic thickness. Wang et al. [11] studied a vibration problem of a generalized variable thickness plate and approximated its vibration equation through the Frobenius method, so as to solving the vibration modal and natural frequency of a variable cross-section beam. Xu et al. [12] studied a method for vibration mode and natural frequency of a variable section beam by an approximate fitting vibration equation with series when the rigidity of the beam is a power function. Tang and Wu [13] used the finite element method to calculate deflections of the parabolic variable section beam and tapered the variable section beam under different constraints. Jang [14] solved the dynamic equation of the beam with periodic variable section through the spectral element method and obtained great precision deflection under the condition of high-frequency vibration. The methods mentioned above have achieved good results in the study of the beam model with specific structures. How to find an analytical method that could be applied to the vibration problem of a more general variable section beam has become the focuses of subsequent research.

Adomian decomposition method (ADM) includes series fitting to carry out multiorder iteration, and thus obtains a high-precision result [15]. ADM could calculate modal problems of the beam with arbitrary variable section theoretically. Haddadpour [16] constructed a modal function of a uniform beam by ADM. With an infinite iteration order, the results from ADM converged to the analytical solution from the traditional method, and then the correctness of ADM was proved. Keshmiri et al. [17] analyzed vibration characteristics of three cantilever beams with different variable sections and obtained the natural frequency through ADM. Mao and Pietrzko [18] derived a method for calculating natural frequency and mode function of the stepped beam based on ADM and verified the accuracy of these results. However, ADM could also have calculation problems for some special structures.

Transfer matrix method (TM) is a kind of theoretical calculation method with strong expansibility. This method is used to associate the components with continuous conditions in a system, so as to achieve the purpose of analyzing the whole system. Fakoukakis and Kyriacou [19] combined the TM with the rigid-flexible mixed multibody system dynamic method to solve the problem that the complex multibody structure is difficult to model accurately at the junction. Fakoukakis and Kyriacou [19] used TM to solve the folding frame structure with equal section and obtained natural frequency, deflection of some points, and bending moment. Cui et al. [20] proposed a semianalytical method for solving modal function and natural frequency of the variable section beam based on TM. However, multiorder matrices are multiplied continuously in the calculation process of this method and then the amount of calculation increases exponentially with matrices increasing. Therefore, in most studies using the semianalytical method, the segment number of the beam can only reach 8 at most, which will limit the further improvement of results' accuracy.

In the process of solving, ADM could obtain high-precision results although there exists the problem of large computation caused by high-order Taylor expansion. If the idea of piecewise solution in TM can be applied, the problem of excessive iteration calculation in the original ADM could be solved effectively. Therefore, the ADM is improved in this paper, and the Adomian decomposition-transfer matrix method (ADTM) is proposed which can be used to solve the mode function and natural frequency of the more general type of the beam with a variable section. The analysis idea of this improved analytic method is that it divides the whole beam into finite sections and builds the mode functions of each section first; then each discrete section is solved by association. The ADTM can not only obtain high-precision results of mode function and natural frequency of the beam with an arbitrary variable section, but also shorten the time required for calculation greatly.

2. Construction of Modal Function

Based on Euler–Bernoulli beam theory, the force analysis of transverse vibration of beams is shown in Figure 1(a). The moment and shear force on the cross section are expressed as $M(x,t)$ and $Q(x,t)$, respectively. L and $y(x,t)$ are the length and bending deflection of the beam, respectively. Force analysis of beam's microsegment dx is performed as shown in Figure 1(b).

The force and moment balance equations could be established according to the D'Alembert's principle. The modal function and natural frequency of the beam could be gained by analyzing free vibration [21, 22]. In free vibration, consider the external load is zero, that is, $q(x,t) = 0$. Then, the vibration function could be written as follows:

$$\rho A(x)\frac{\partial^2 y(x,t)}{\partial t^2} + \frac{\partial^2}{\partial x^2}\left[EI(x)\frac{\partial^2 y(x,t)}{\partial x^2}\right] = 0, \tag{1}$$

where $\rho A(x)$ and $EI(x)$ are the mass per unit length and the flexural rigidity of the beam, respectively.

The Galerkin method is used to discretize the deflection function:

$$y(x,t) = \sum_{i=1}^{\infty} u_i(t)\phi_i(x). \tag{2}$$

Substituting equation (2) into equation (1) gives the following:

$$EI(x)\frac{d^4\phi_i(x)}{dx^4} + 2EI'(x)\frac{d^3\phi_i(x)}{dx^3} + EI''(x)\frac{d^2\phi_i(x)}{dx^2} + \frac{\ddot{u}_i(t)}{u_i(t)}\rho A(x)\phi(x) = 0, \tag{3}$$

where $EI'(x) = dEI(x)/\mathrm{d}x$, $\ddot{u}(t) = \mathrm{d}^2u(t)/\mathrm{d}t^2$, and i is the modal order. According to the orthogonality of modes,

$$\frac{\ddot{u}_i(t)}{u_i(t)} = -\omega_i^2. \tag{4}$$

By substituting equation (4) into equation (3), the following results are obtained:

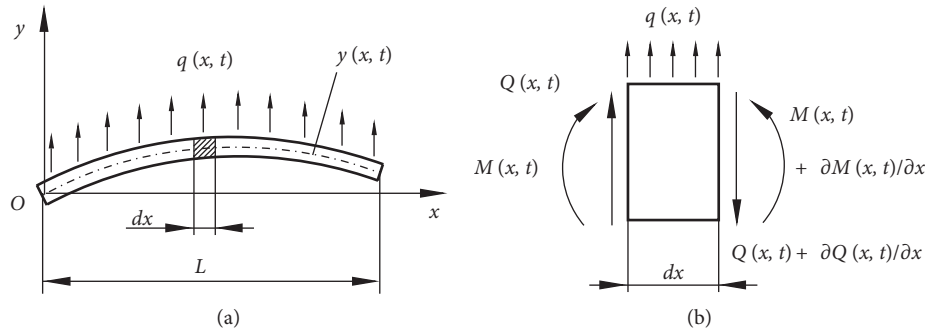

Figure 1: Force analysis of the Euler–Bernoulli beam. (a) Beam structure. (b) Microsegment dx.

$$L_x[\phi(x)] = -2f_1(x)\phi'''(x) - f_2(x)\phi''(x) + \omega_1^2 f_3(x)\phi(x), \tag{5}$$

where $L_x = \mathrm{d}^4/\mathrm{d}x^4$ and

$$f_1(x) = \frac{EI'(x)}{EI(x)},$$
$$f_2(x) = \frac{EI''(x)}{EI(x)}, \tag{6}$$
$$f_3(x) = \frac{\rho A(x)}{EI(x)}.$$

By integrating both sides of equation (5) the following relation is obtained:

$$\phi(x) - \phi(x_0) - x\phi'(x_0) - \frac{x^2}{2}\phi''(x_0) - \frac{x^3}{6}\phi'''(x_0) = -L_\xi^{-1}\left[2f_1(x)\phi'''(x) + f_2(x)\phi''(x) - \omega_i^2 f_3(x)\phi(x)\right], \tag{7}$$

where x_0 is the coordinate value of the x-axis at the beginning of the beam and L_x^{-1} is the quadruple integral operator of the interval $[x_0, x]$. Obviously, $\phi(x_0)$, $\phi'(x_0)$, $\phi''(x_0)$, and $\phi'''(x_0)$ are constants. Let $A = \phi(x_0)$, $B = \phi'(x_0)$, $C = \phi''(x_0)$, and $D = \phi'''(x_0)$.

Building the iterative modal function [16] of a general beam, and then the relations could be obtained as follows:

$$\phi(x) = \sum_{j=0}^{n} \phi_j(x), \tag{8}$$

$$\phi_0 = A + Bx + C\frac{x^2}{2} + D\frac{x^3}{6}, \tag{9}$$

$$\phi_j(x) = -L_x^{-1}\left[2f_1(x)\phi'''_{j-1}(x) + f_2(x)\phi''_{j-1}(x) - \omega_i^2 f_3(x)\phi_{j-1}(x)\right]. \tag{10}$$

In equation (8), n is the iterative order of ADM. The higher the value of n is, the higher the precision of mode function is.

As shown in equation (6), $f_i(x)$ $(i = 1, 2, 3)$ are functions of x [17]. Then, equivalent functions $f_1(x)$ and $f_2(x)$ could be viewed as $1/x$ and $1/x^2$, respectively. $f_3(x)$ can be rewritten as follows:

$$f_3(x) = \left(\frac{\rho}{E}\right)\frac{A(x)}{I(x)} = \left(\frac{\rho}{12E}\right)\frac{1}{h^2(x)}, \tag{11}$$

where $h(x)$ is the thickness of the beam. Then, the equivalent function of $f_3(x)$ could be considered as $1/x^{2r}$. That means that r is the power of $h(x)$'s equivalent power function. Therefore, it could be seen that equation (10) cannot be integrated directly because $f_1(x)$, $f_2(x)$, and $f_3(x)$ are contained in the quadruple integral L_x^{-1}. Thus, Taylor expansion is introduced for approximate fitting [8], and equation (11) can be transformed into

$$\phi_j(x) = -L_x^{-1}\left[2T_1(x)\phi'''_{j-1}(x) + T_2(x)\phi''_{j-1}(x) - \omega_i^2 T_3(x)\phi_{j-1}(x)\right], \tag{12}$$

where $T_1(x)$, $T_2(x)$, and $T_3(x)$ are the fitting functions of $f_1(x)$, $f_2(x)$, and $f_3(x)$, respectively.

3. Discussion of Fitting Error

The original ADM is applied to discuss the fitting error of beams with different sections under the same order expansion. Taylor fitting calculation has unavoidable defects, which is the fitting error becomes larger when it is away from the expansion base point. If the error needs to be reduced, it should be increased in the order of expansion and then the term of expansion is also increased. According to the iterative character of the ADM method, the expansion term of the fitting function is multiplied continuously in the iterative process, which will lead to huge calculation. In the finite order, there will be some fitting errors between the fitting function and the original function.

Taking $f_1(x)$ as an example, the analysis of $f_2(x)$ and $f_3(x)$ is similar. As the fitting function is farther away from the expansion base point, the fitting error is larger. To reduce the fitting error, a new expansion base point is set to O', which is the midpoint of the beam, as shown in Figures 2(a) and 2(b). Then, the error between the original $f_1(x)$ and the fitting function $T_1(x)$ should be expressed as $\eta(x) = T_1(x) - f_1(x)$.

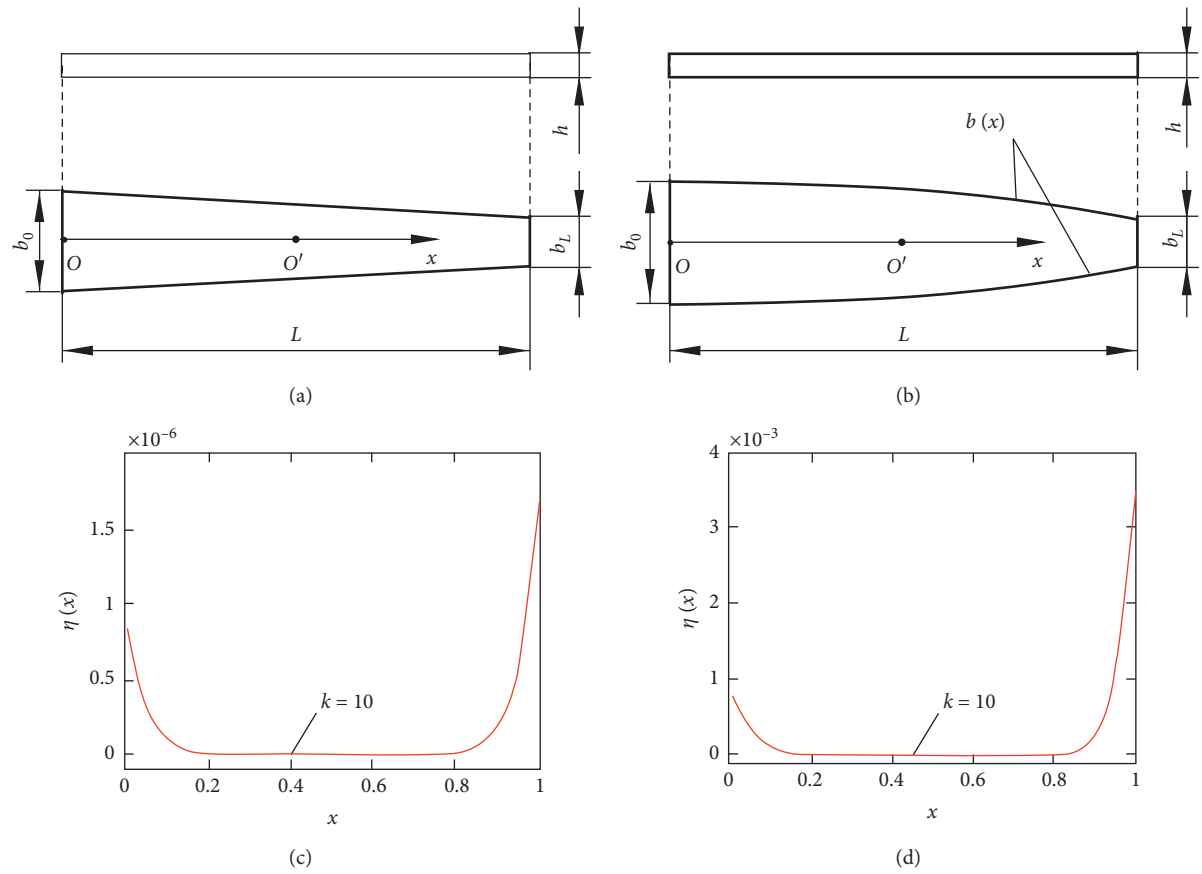

FIGURE 2: Structure model and fitting error $\eta(x)$ when $b_0 = 0.2$, $b_L = 0.08$, $L = 1$, and $h = 0.015$. (a) Trapezoidal beam. (b) Trapezoidal convex beam with width function $b(x) = b_0 - (b_0 - b_L)(x/L)^2$. (c-d) Taylor fitting error of models (a) and (b), respectively.

In Figures 2(c) and 2(d), k is the order of Taylor expansion. It could be seen that different section functions have a great influence on the fitting error under the same expansion order. When $k = 10$, the difference between the fitting error of the trapezoidal beam in Figure 2(a) and that of the trapezoidal convex beam in Figure 2(b) is three orders of magnitude. If the above two fitting errors are on the same order of magnitude, then k in the case of the trapezoidal convex beam needs to reach the 26-th order. And, that leads to the computation problem caused by Taylor's higher-order fitting that was mentioned earlier.

In order to reveal more intuitively the influence of Taylor fitting on the calculation quantity of ADM, the calculation quantity is simply estimated now. Because the Taylor fitting order k equals the number of expansion terms, it also takes into account that the number of terms will be multiplied once in each iteration. Therefore, the number of calculation terms generated by ADM can be expressed as k_n. It can be seen that the variation of the expansion order k will have a great influence on the calculation of the iteration part.

In addition, it can be found also that in some cases even though the order of Taylor series is up to $k = 200$, the section function still cannot be fitted, as shown in Figure 3. When the beam with a variable section is of the Timoshenko function, that is, the trapezoidal concave beam, the width function is $b(x) = b_0 - (b_0 - b_L)((2xt - nL)/L)^2$. If $b_m \le 1$, Taylor expansion cannot be completed. Obviously, it is almost impossible to substitute the fitting function $T_1(x)$ with $k = 200$ into the equations (8), (9), and (12) for iterative computations. Therefore, in practical application, ADM is limited by the expansion order k of the fitting function, so it cannot be fully applied to solve the arbitrary section beam.

4. Segmentation and Fitting

In order to solve the problems of excessive calculation amount and failure mentioned above, a new analytical calculation method, ADTM, is proposed in this paper. The proposed method could divide the whole structure into some segments, and then length of each segment is smaller than the overall length. In this way, it could solve the disadvantage of fitting functions $T_1(x)$, $T_2(x)$, and $T_3(x)$ because of the distance from the base point of expansion, which is caused by the original algorithm. The modal function and natural frequency of the whole structure could be obtained by correlating each segment through the continuity condition in turn.

Firstly, divide the whole structure into p segments according to the section function of the whole structure, as shown in Figure 4. Then, the modal functions of each section could be established by using equations (8), (9), and (12), respectively. Therefore, they could be rewritten as follows:

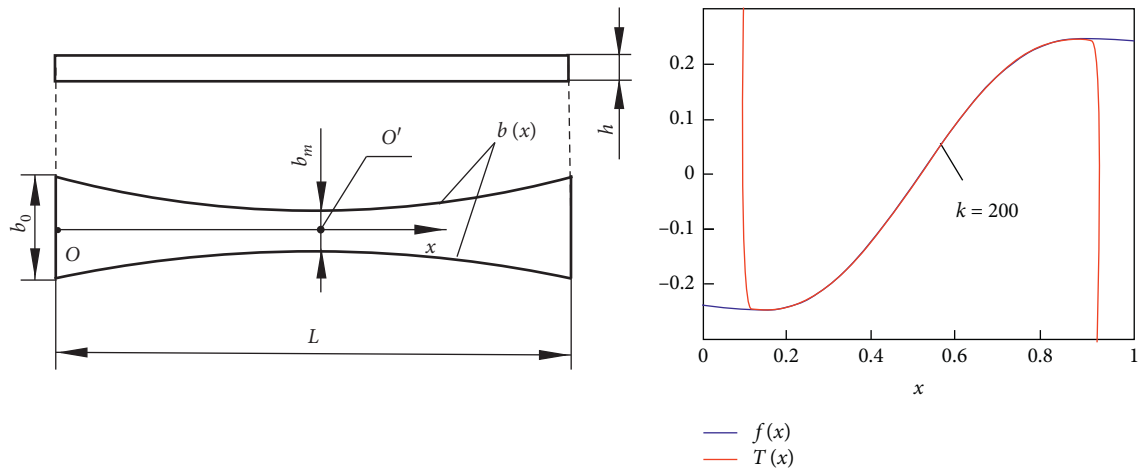

(a) (b)

Figure 3: Failure example of ADM. (a) Concave beam with width function $b(x) = b_0 - (b_0 - b_L)((2xt - nL)/L)^2$. (b) Comparison of the original $f(x)$ and the fitting function $T(x)$.

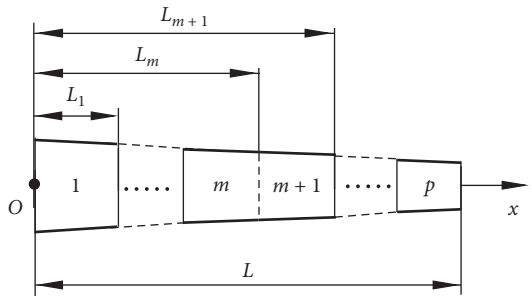

Figure 4: Whole structure with p segments.

$$\phi_{(m)}(x) = \sum_{j=0}^{n} \phi_{j(m)}(x), \tag{13}$$

$$\phi_{0(m)} = A_{(m)} + B_{(m)}x + C_{(m)}\frac{x^2}{2} + D_{(m)}\frac{x^3}{6}, \tag{14}$$

$$\phi_{j(m)}(x) = -L_x^{-1}\left[2T_1\phi'''_{j-1(m)}(x) + T_2(x)\phi''_{j-1(m)}(x) - \omega_i^2 T_3(x)\phi_{j-1(m)}(x)\right], \tag{15}$$

where $L_m \le x \le L_{m+1}$, $j \ge 0, m = 1, 2, \ldots, p$. After n-order iteration of equation (15), several modal functions with five unknown parameters could be obtained, which are expressed as follows:

$$\phi_{(m)}(x) = H_{A(m)}A_{(m)} + H_{B(m)}B_{(m)} + H_{C(m)}C_{(m)} + H_{D(m)}D_{(m)}, \tag{16}$$

where $H_{A(m)}, H_{B(m)}, H_{C(m)}$, and $H_{D(m)}$ contain variable x and the undetermined parameter $\omega_{i(m)}$.

Natural frequency is the inherent property of the whole structure. Then, the natural frequencies of the monolithic structure before and after the section are the same, which can be expressed as $\omega_i = \omega_{i(1)} = \omega_{i(2)} =, \cdots, = \omega_{i(p)}$. According to the continuity condition, the displacement, angle, bending moment, and shear force on the right section of the m-th segment are equal to that on the left section of the $(m+1)$-th segment. Therefore, the following relationships are satisfied:

$$\phi_{(m)}(L_m) = \phi_{(m+1)}(L_m), \tag{17}$$

$$\phi'_{(m)}(L_m) = \phi'_{(m+1)}(L_m), \tag{18}$$

$$EI(L_m)\phi''_{(m)}(L_m) = EI(L_m)\phi''_{(m+1)}(L_m), \tag{19}$$

$$\left[EI\left(L_{(m)}\right)\phi''_{(m)}(L_m)\right]' = \left[EI\left(L_{(m)}\right)\phi''_{(m)}(L_m)\right]'. \tag{20}$$

Substituting equation (16) into equations (17)–(20), the following iteration equations can be obtained:

$$Z_m(L_m) \cdot P_m = Z_{m+1}(L_m) \cdot P_{m+1}, \tag{21}$$

where

$$P_m = \left[A_{(m)} \;\; B_{(m)} \;\; C_{(m)} \;\; D_{(m)}\right]^T. \tag{22}$$

The relationship between both sides of iteration (21) shows that this equation is transitive, and the transformation can be obtained as follows:

$$Z \cdot P_1 = P_p, \tag{23}$$

where

$$Z = \left[Z_p^{-1}\left(L_{p-1}\right) \cdot Z_{p-1}\left(L_{p-1}\right)\right] \ldots \left[Z_{m+1}^{-1}\left(L_m\right) \cdot Z_m\left(L_m\right)\right] \ldots \left[Z_3^{-1}\left(L_2\right) \cdot Z_2\left(L_2\right)\right]\left[Z_2^{-1}\left(L_1\right) \cdot Z_1\left(L_1\right)\right], \tag{24}$$

$$Z_m = \begin{bmatrix} H_{A(m)} & H_{B(m)} & H_{C(m)} & H_{D(m)} \\ H''_{A(m)} & H''_{B(M)} & H''_{C(m)} & H''_{D(m)} \\ EI(x)H''_{A(m)} & EI(x)H''_{B(M)} & EI(x)H''_{C(m)} & EI(x)H''_{D(m)} \\ \left[EI(x)H''_{A(m)}\right]' & \left[EI(x)H''_{B(M)}\right]' & \left[EI(x)H''_{C(m)}\right]' & \left[EI(x)H''_{D(m)}\right]' \end{bmatrix}. \tag{25}$$

$[Z_{m+1}^{-1}(L_m) \cdot Z_m(L_m)]$ in equation (24) represents the transfer relationship between the m-th segment and the $(m+1)$-th segment and can be considered as a function of the natural frequency ω. Taking the cantilever beam as an example, the four boundary conditions are given as follows:

$$\begin{aligned} \phi_{(1)}(0) &= 0, \\ \phi'_{(1)}(0) &= 0, \\ \phi''_{(p)}(L) &= 0, \\ \phi'''_{(p)}(L) &= 0. \end{aligned} \tag{26}$$

Then, substituting equation (26) into equation (16), we have

$$\begin{aligned} \Lambda_1 P_1 &= 0, \\ \Lambda_p P_p &= 0, \end{aligned} \tag{27}$$

where

$$\begin{aligned} \Lambda_1 &= \begin{bmatrix} H_{A(1)} & H_{B(1)} & H_{C(1)} & H_{D(1)} \\ H'_{A(1)} & H'_{B(1)} & H'_{C(1)} & H'_{D(1)} \end{bmatrix}_{x=0}, \\ \Lambda_p &= \begin{bmatrix} H''_{A(p)} & H''_{B(p)} & H''_{C(p)} & H''_{D(p)} \\ H'''_{A(p)} & H'''_{B(p)} & H'''_{C(p)} & H'''_{D(p)} \end{bmatrix}_{x=L}. \end{aligned} \tag{28}$$

Combining equations (24) and (27), the following could be obtained:

$$\begin{bmatrix} \Lambda_1 \\ \Lambda_p Z \end{bmatrix} P_1 = 0. \tag{29}$$

The left side of equation (29) is a 4×4 matrix. If there is a nonzero solution to the equation, then

$$\det\begin{bmatrix} \Lambda_1 \\ \Lambda_p Z \end{bmatrix} = 0, \tag{30}$$

where det(•) represents the determinant of the matrix. The natural frequency ω can be calculated by equation (30). Then, substituting ω into equation (29), the coefficient P_1 of the first segment is derived. Then, both ω and P_1 are substituted into the iterative equation (21), and the iterative solution is carried out successively. According to the above steps, the modal function $\phi_{(m)}(x)$ of all segments can be obtained.

Parameter p, which is the number of segments, is directly proportional to the fitting accuracy of fitting functions $T_1(x)$, $T_2(x)$, and $T_3(x)$ that have a little impact on the calculated amount of the method itself. From equations (24) and (26), it can be seen that the transfer function Z could be obtained by multiplying $2p$ matrices that are 4×4, which leads that the increase in p will cause the computation of Z to increase rapidly. This problem can be solved by analyzing the fitting error of each segment's fitting function. Therefore, when segmenting, the fitting error could be in the same order of magnitude by adjusting the length of each segment, so as to reduce the number of segments p. According to experience, the whole structure could be generally divided into three sections for calculation, which is enough to solve most of the variable section structures commonly encountered. If the variation of the section function is particularly complex, the number of segments should be selected according to the variation rule.

5. Examples

In this section, the cantilever structure is taken as an example to verify the excellence of ADTM by comparing the results obtained by several different methods. What needs illustration is that both ADM and ADTM are used to approximate the modal function and natural frequency by series expansion, so there are two kinds of errors in both methods when they are used to solve vibration equations. One is the truncation error caused by the finite series expansion of the method itself; the other is the fitting error caused by the Taylor series introduced in equation (12). Therefore, the overall error of the method involves the accumulation of both the errors.

5.1. Uniform Beam. The unit mass and stiffness of the uniform beam are constant, so there is no Taylor fitting error term, when ADM or ADTM is used to solve the vibration equation. Then, the solution error is only caused by the truncation of the series expansion of the method itself. Table 1 shows the results of the first three natural frequencies of uniform beams from different methods. Consider physical parameters as follows: length $L = 1$, width $b = 0.2$, thickness $h = 0.015$, and elastic modulus $E = 7.1 \times 10^{10}$.

In Table 1, the theoretical result is the complete solution by using the traditional method. It also can be seen that the results of both methods are gradually close to theoretical results with the iterative order increasing. However, the result of the higher-order natural frequency has more error than that of the lower-order natural frequency, which makes ADM unable to solve in the lower-order iteration.

Table 1: Comparison of results from ADTM and ADM in the uniform beam case.

Frequency	Order of iteration	ADM	ADTM		FEM result	Theoretical result
			($p = 2$)	($p = 3$)		
ω_1	$n = 1$	79.0341	78.2747	78.1178	77.7096	78.0726
	$n = 2$	78.0743	78.0727	78.0726		
	$n = 3$	78.0726	78.0726	78.0726		
Ω_2	$n = 1$	417.6492	454.8542	492.8109	487.1444	489.2727
	$n = 2$	456.9292	488.6935	489.2750		
	$n = 3$	488.3615	489.2715	489.2727		
Ω_3	$n = 1$	—	1290.2621	1309.2891	1362.8536	1369.9775
	$n = 2$	—	1350.1889	1365.6756		
	$n = 3$	1095.9032	1369.6495	1369.9640		

Under the same condition and iteration order n, the result from ADTM has a higher precision than ADM. Moreover, the number of segments of ADTM also affects accuracy. Comparing results with $p = 2$ and $p = 3$, it is obvious that the accuracy of the latter is higher than that of former under the same n.

By using the natural frequency obtained in Table 1, the corresponding modal function can also be obtained, which is shown in Figure 5 through ADTM with $n = p = 3$. For the convenience of errors analysis, the dimensionless transforms are given as follows:

$$\hat{x} = \frac{x}{L}, \qquad \hat{\phi}_i = \frac{\phi_i}{\phi_i(L)}. \tag{31}$$

In order to understand more clearly, the error can be expressed as

$$\eta_{\phi_i} = \hat{\Phi}_i(\hat{x}) - \hat{\phi}_i(\hat{x}), \tag{32}$$

where $\hat{\Phi}_i(\hat{x})$ is the theoretical results of modal function and $\hat{\phi}_i(\hat{x})$ is an approximate modal function obtained by ADM or ADTM.

Generally speaking, errors from different methods are not in the same order of magnitude. Figure 6 shows the modal function's error η_ϕ of the first three natural frequencies represented by logarithmic coordinate axes under different methods. It can be seen that whether $p = 2$ or $p = 3$, the results from ADTM show better fitting accuracy than that from ADM in any modals under the same condition of iteration order $n = 3$. In addition, the errors of first modal fitting from both methods are in the same order of magnitude. In the second modal, whether $p = 2$ or $p = 3$, the errors from ADTM are about 3 or 5 orders of magnitude less than that from ADM. The error accuracy of the third modal function is similar to the second.

In addition, the experimental method is also used to further verify the modal solved by ADTM. Figure 7 shows the ADTM results of the dimensionless vibration modal and amplitude frequency response comparing with experimental data, respectively. In Figure 7, the ADTM results are basically in agreement with the experimental data, and the max error of the resonance peak is less than 3.5% in Figure 7(b). Therefore, the effectiveness and accuracy of the ADTM are proved by the above theoretical and experimental analysis.

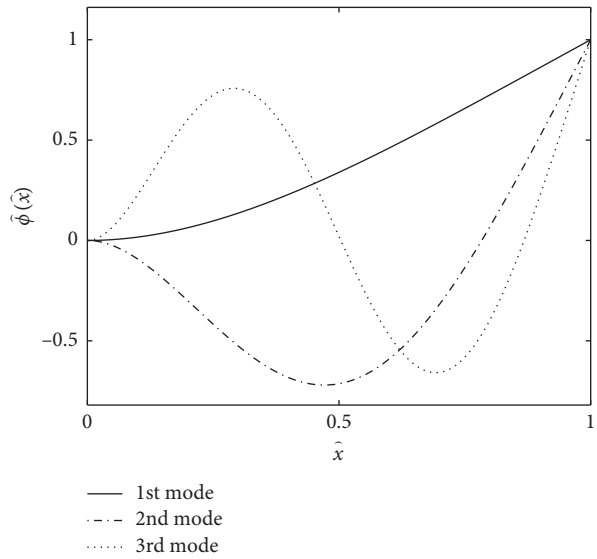

Figure 5: The first three modal functions obtained by ADTM with $n = p = 3$.

5.2. Trapezoidal Convex Beam. The trapezoidal convex beam mentioned in Figure 2(b) is analyzed. Both analytical methods are used, and the results are shown in Table 2. When using ADM, the order of Taylor expansion is $k = 26$; when using ADTM, the beam is divided into three segments firstly, as shown in Figure 8(a), and the order of expansion is $k_1 = 10$, $k_2 = 10$, and $k_3 = 11$, respectively. The comparison of the fitting error before and after segmentation is shown in Figure 8(b). The blue, cyan, and green curves correspond to the first, second, and third segments, respectively. It is obvious that three fitting error curves are close to zero. However, when the original ADM is applied to directly fit this structure as a whole, the fitting errors at both ends of this structure are much larger than that at the middle. Therefore, the accuracy of the proposed ADTM could be proved again.

In Table 2, when the same iteration order n is used, the natural frequency results of ADTM are closer to the finite element simulation (FEM) in Table 3 than those of the original ADM. At $n = 5$, the results from ADM have not yet

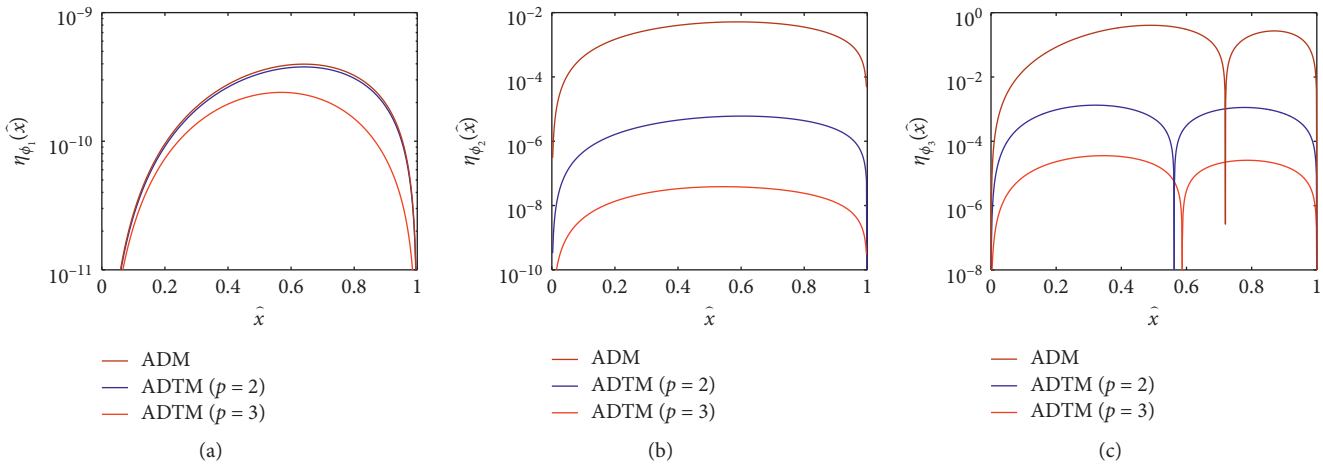

Figure 6: The errors of modal functions from different methods. (a) First modal, (b) second modal, and (c) third modal.

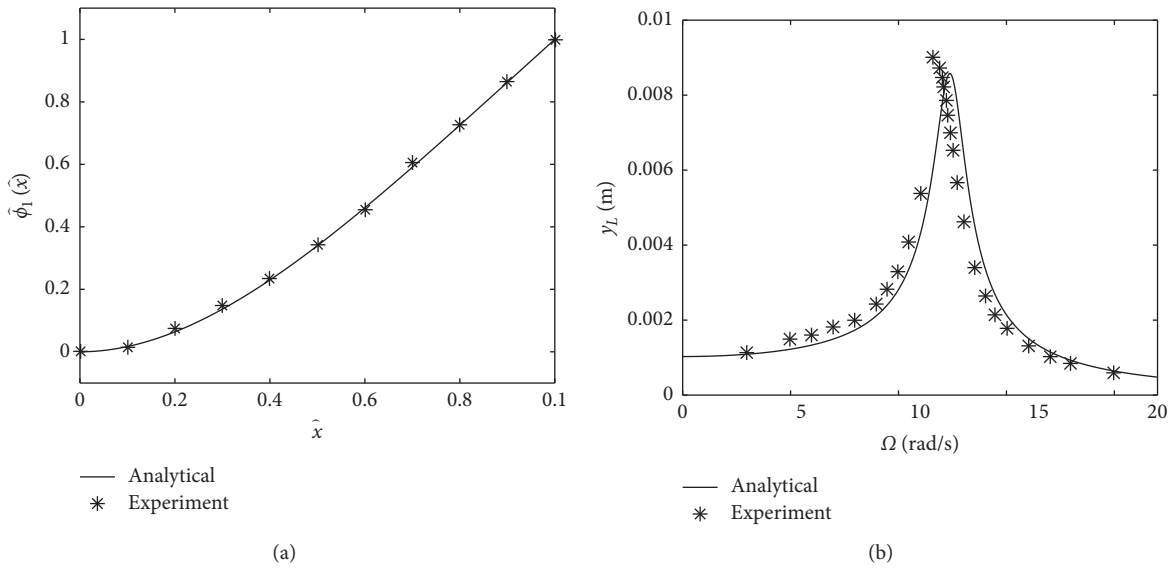

Figure 7: Comparison of ADTM and experimental results. (a) Vibration modal. (b) Amplitude frequency response.

Table 2: Comparison of results from ADTM and ADM in the trapezoid convex beam case.

	ADM ($k = 26$)			ADTM ($p = 3$, $k_1 = 10$, $k_2 = 10$, $k_3 = 11$)		
Order of iteration	ω_1 (rad/s)	ω_2 (rad/s)	ω_3 (rad/s)	ω_1 (rad/s)	ω_2 (rad/s)	ω_3 (rad/s)
$n = 5$	101.1648	502.4120	1349.6159	99.2913	533.8116	1420.8928
$n = 6$	99.8467	523.7288	1527.6533	99.2814	533.8033	1420.9502
$n = 7$	99.4269	531.2438	1347.9822	99.2802	533.8025	1420.9597
$n = 8$	99.3134	533.2523	1455.0812	99.2801	533.8025	1420.9609
$n = 9$	99.2868	533.6983	1426.7344	99.2801	533.8024	1420.9610
$n = 10$	99.2813	533.7847	1421.9121	99.2801	533.8024	1420.9610

converged to 10° order of magnitude; in contrast, the result from ADTM converges rapidly to 10^{-1} order of magnitude, and the calculation speed is 2.5 times faster than that of the traditional method. From the point of view of the convergence radius, if the result is converged to 10^{-2} order of magnitude, the iteration order of the traditional method needs to reach $n = 9$, but the iteration order of ADTM only needs $n = 6$. Moreover, the calculation speed of ADTM is

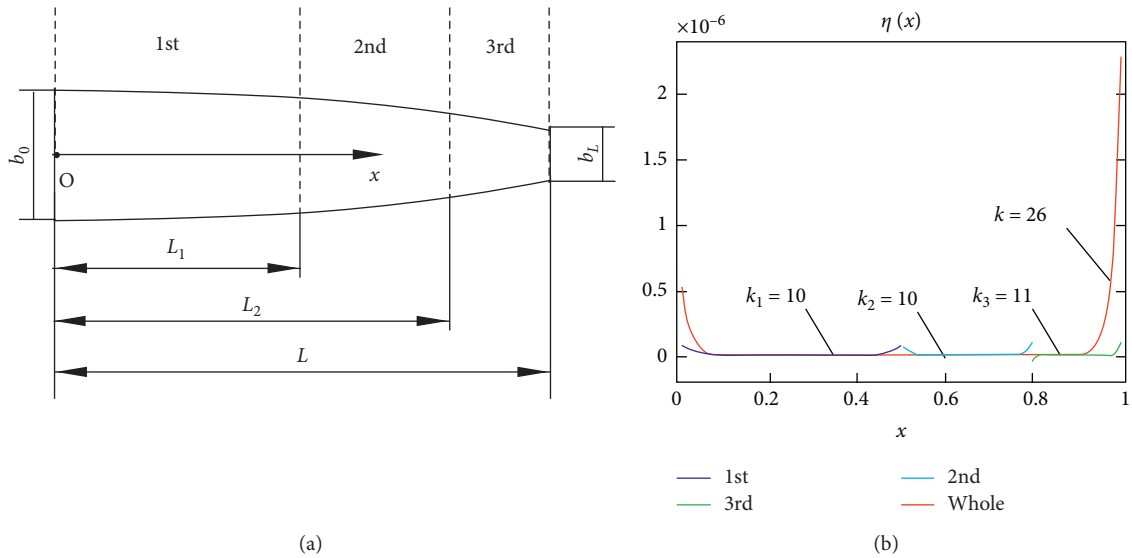

Figure 8: Analysis of the trapezoid convex beam. (a) Structure model. (b) Error comparison of ADTM and ADM.

Table 3: Comparison of results from various methods in four cases.

Beam model	Frequency	FEM	ADTM ($n = 10$, $p = 3$, $k_1 = 10$, $k_2 = 10$, $k_3 = 11$)		ADM ($n = 26$, $k = 10$)		Semianalytical method ($p = 8$)	
		Result (rad/s)	Result (rad/s)	Error (‰)	Result (rad/s)	Error (‰)	Result (rad/s)	Error (‰)
Trapezoidal beam	ω_1	102.1261	101.8169	3.0	101.8159	3.0	101.3213	7.9
	ω_2	535.4677	533.3845	3.9	533.3869	3.9	530.4472	9.4
	ω_3	1423.3859	1415.5921	5.4	1415.5946	5.5	1407.6242	11.1
Trapezoidal convex beam	ω_1	99.5983	99.2801	3.1	99.2813	3.1	98.7987	8.1
	ω_2	536.2030	533.8025	4.5	533.7847	4.5	530.2409	11.1
	ω_3	1428.8301	1420.9610	5.5	1421.9121	4.8	1410.5328	12.8
Concave beam	ω_1	73.9735	74.2340	3.5	—	—	74.5634	7.9
	ω_2	499.8834	497.9771	3.8	—	—	496.4176	6.9
	ω_3	1385.9541	1378.6030	5.3	—	—	1374.8716	7.9

about 6.5 times faster than that of the traditional method. Therefore, the calculation process of the proposed method significantly improves iteration efficiency and greatly reduces the overall calculation time.

5.3. Trapezoidal Concave Beam. The concave section beam cannot be calculated by ADM that is mentioned above and shown in Figure 3. In order to illustrate the effectiveness and accuracy of the proposed method further, the ADTM is compared with the semianalytical method [23] for such a structure model, and then the results are listed in Table 4. When using ADTM, there are three schemes of segmentation. Case one, $p = 2$, $k_1 = 11$, and $k_2 = 11$; case two, $p = 3$, $k_1 = 10$, $k_2 = 10$, and $k_3 = 11$; case three, $p = 4$, $k_1 = 11$, $k_2 = 10$, $k_3 = 10$, and $k_4 = 11$.

In Table 4, it can be seen that the results from ADTM converge to 74.23 finally in each segmentation case, with the increase in the iteration order n. And, the results from the semianalytical method converge to ADTM with the number of segments p increasing. Therefore, it is proved that the ADTM has a better precision.

5.4. Trapezoidal Beam. In order to illustrate the general applicability of the proposed method, three methods are used to solve the more common trapezoid beam, as shown in Figure 2(a). The results from ADTM and ADM are shown in Table 5, and the results from ADTM and the semianalytical method are shown in Table 3. The accuracy of those three methods is discussed by comparing with the finite element modal analysis, and all results are listed in Table 3.

In Table 5, when $n = 5$, the result of the natural frequency obtained by ADM converges to the 10° order of magnitude; the result from ADTM converges to the 10^{-2} order of magnitude, and the calculation speed is twice than that of ADM. From the point of view of the convergence radius, if the result converges to the 10^{-2} order of magnitude, then the iterative order of ADM needs to be $n = 10$ and that of ADTM only needs to be $n = 5$. Moreover, the calculation speed of

Table 4: Comparison of results from ADTM and the semianalytical method in the trapezoid concave beam case.

Segments	Order of iteration	ADTM			Semianalytical method		
		ω_1 (rad/s)	ω_2 (rad/s)	ω_3 (rad/s)	ω_1 (rad/s)	ω_2 (rad/s)	ω_3 (rad/s)
$p = 2$	$n = 6$	73.5041	491.8213	1362.2632	78.0726	489.2727	1369.9777
	$n = 8$	74.1666	497.3769	1372.2632			
	$n = 10$	74.2328	497.3795	1376.9487			
$p = 3$	$n = 6$	74.7595	497.1698	1377.4637	76.4328	488.4799	1350.0823
	$n = 8$	74.2509	497.9426	1378.4681			
	$n = 10$	74.2340	497.9771	1378.6030			
$p = 4$	$n = 6$	74.6325	497.3214	1378.1042	75.5023	495.5865	1355.1130
	$n = 8$	74.2414	497.9611	1378.5935			
	$n = 10$	74.2337	497.9768	1378.6141			

Table 5: Comparison of results from ADTM and ADM in the trapezoid beam case.

	ADM ($k = 26$)			ADTM ($p = 3$, $k_1 = 10$, $k_2 = 10$, $k_3 = 11$)		
Order of iteration	ω_1 (rad/s)	ω_2 (rad/s)	ω_3 (rad/s)	ω_1 (rad/s)	ω_2 (rad/s)	ω_3 (rad/s)
$n = 5$	101.1324	536.5036	1598.5717	101.8157	533.3674	1415.5740
$n = 6$	101.6175	534.5213	1497.6120	101.8161	533.3827	1415.5901
$n = 7$	101.7673	533.6933	1424.1163	101.8162	533.3844	1415.5919
$n = 8$	101.8057	533.4538	1416.5559	101.8162	533.3846	1415.5921
$n = 9$	101.8142	533.3980	1415.6736	101.8162	533.3846	1415.5921
$n = 10$	101.8159	533.3869	1415.5946	101.8162	533.3846	1415.5921

Table 6: Comparison of results from ADTM and the semianalytical method in the trapezoid beam case.

	ADTM ($n = 10$)			Semianalytical method		
Segments	ω_1 (rad/s)	ω_2 (rad/s)	ω_3 (rad/s)	ω_1 (rad/s)	ω_2 (rad/s)	ω_3 (rad/s)
$p = 2$	101.8150	533.3786	1415.5773	94.4962	496.5471	1373.9867
$p = 3$	101.8162	533.3827	1415.5901	98.4109	514.6177	1370.6740
$p = 4$	101.8162	533.3828	1415.5902	99.8686	522.2463	1387.4444

ADTM is 17 times than that of ADM. In Table 6, three segmentation schemes of ADTM are the same as those in Table 2. When $p = 2$, the result from the semianalytical method has a large error, and the result from ADTM converges to the 10^{-2} order of magnitude. When $p > 2$, the result from ADTM converges to the 10^{-5} order of magnitude. Moreover, the result from the semianalytical method converges to that from ADTM with p increasing.

The results of the four examples above are compared together and listed in Table 3. At this time, the semianalytical method takes the highest number of segments in conventional research, that is, $p = 8$. The results show that the errors from ADTM are all smaller than that from the semianalytical method in every example. In addition, the errors from ADTM are still low in the example of ADM method failure. Therefore, the general applicability and high accuracy of ADTM are demonstrated.

6. Conclusion

In this paper, a new analytical method ADTM is proposed to solve modal function and natural frequency of a beam with a variable section. The proposed method could effectively combine advantages of high accuracy and fast calculation. Firstly, the uniform beam is analyzed to verify the correctness of the proposed method. The results from ADTM, the complete solution, FEM, and experiment are compared to show the accuracy of ADTM. Then, the excellent calculation accuracy and convergence of the ADTM are proved by comparing the results from different analytical methods with those of FEM under several typical examples. Compared with the ADM, the calculation time is shorter and the solution accuracy is higher by using the proposed method. In addition, some special structure models with a variable section which cannot be solved by ADM could also be analyzed. It is also further proved that ADTM is more universal for the excellent results.

The ADTM method is not restricted by traditional modal analytical methods. Based on the same principle, the modal functions and natural frequencies of the arbitrary variable sectioned structure under longitudinal, torsional, and bending coupled torsional vibration could be derived, and the influence of geometric nonlinearity of axial force applying on the beam with a variable section could be analyzed effectively.

Data Availability

The data used to support the findings of this study are included within the article.

Conflicts of Interest

The authors declare that they have no conflicts of interest.

Acknowledgments

The authors gratefully acknowledge the support of the National Natural Science Foundation of China (Grant nos. 11602169, 11702188, 11772218, 11702192, and 51605330), the Natural Science Foundation of Tianjin City (Grant nos. 17JCYBJC18900 and 18JCYBJC19900), and the Scientific Research Project of Tianjin Municipal Education Commission (Grant no. 2017KJ262).

References

[1] B. L. Ooi, J. M. Gilbert, and A. R. A. Aziz, "Analytical and finite-element study of optimal strain distribution in various beam shapes for energy harvesting applications," *Acta Mechanica Sinica*, vol. 32, no. 4, pp. 670–683, 2016.

[2] K. Savarimuthu, R. Sankararajan, N. A. M. Gulam, and M. Ani Melfa Roji, "Design and analysis of cantilever based piezoelectric vibration energy harvester," *Circuit World*, vol. 44, no. 2, pp. 78–86, 2018.

[3] J. J. Wang, D. X. Cao, and M. H. Yao, "Dynamic characteristic analysis of piezoelectric energy harvester with variable cross-section cantilever beam," *Piezoelectrics and Acoustooptics*, vol. 40, no. 5, pp. 92–96, 2018.

[4] P. C. Y. Lee and J. Wang, "Piezoelectrically forced thickness-shear and flexural vibrations of contoured quartz resonators," *Journal of Applied Physics*, vol. 79, no. 7, pp. 3411–3422, 1996.

[5] X. Xiong and S. Wang, "Analysis and research of externally prestressed concrete beam vibration behavior," *Earthquake Engineering & Engineering Vibration*, vol. 25, no. 2, pp. 56–61, 2005.

[6] J. N. Reddy, "Nonlocal theories for bending, buckling and vibration of beams," *International Journal of Engineering Science*, vol. 45, no. 2–8, pp. 288–307, 2007.

[7] R. L. Tian, Z. J. Zhao, and Y. Xu, "Variable scale-convex-peak method for weak signal detection," *Science China Technological Sciences*, vol. 63, pp. 1–10, 2020.

[8] J. Wang, "Generalized power series solutions of the vibration of classical circular plates with variable thickness," *Journal of Sound and Vibration*, vol. 202, no. 4, pp. 593–599, 1997.

[9] A. Pielorz and W. Nadolski, "Non-linear vibration of a cantilever beam of variable cross-section," *ZAMM - Journal of Applied Mathematics and Mechanics/Zeitschrift für Angewandte Mathematik und Mechanik*, vol. 66, no. 3, pp. 147–154, 1986.

[10] P. A. A. Laura, R. H. Gutierrez, and R. E. Rossi, "Free vibrations of beams of bilinearly varying thickness," *Ocean Engineering*, vol. 23, no. 1, pp. 1–6, 1996.

[11] J. Wang, P. C. Y. Lee, and D. H. Bailey, "Thickness-shear and flexural vibrations of linearly contoured crystal strips with multiprecision computation," *Computers & Structures*, vol. 70, no. 4, pp. 437–445, 1999.

[12] T. F. Xu, T. Y. Xiang, and R. D. Zhao, "Series solution of natural vibration of variable cross-section Euler-Bernoulli beam under axial force," *Journal of Vibration and Shock*, vol. 26, no. 11, pp. 99–101, 2007.

[13] H. T. Tang and X. Y. Wu, "Analysis of transfer matrix of non-uniform beam based on finite element method," in *Proceedings of the International Conference on Computer Science and Information Processing (CSIP)*, Xi'an, china, August 2012.

[14] T. S. Jang, "A general method for analyzing moderately large deflections of a non-uniform beam: An infinite Bernoulli-Euler-von Kármán beam on a nonlinear elastic foundation," *Acta Mechanica*, vol. 225, no. 7, pp. 1967–1984, 2014.

[15] G. Adomian, R. Rach, and N. T. Shawagfeh, "On the analytic solution of the lane-emden equation," *Foundations of Physics Letters*, vol. 8, no. 2, pp. 161–181, 1995.

[16] H. Haddadpour, "An exact solution for variable coefficients fourth-order wave equation using the Adomian method," *Mathematical and Computer Modeling*, vol. 44, no. 11-12, pp. 1144–1152, 2006.

[17] A. Keshmiri, N. Wu, and Q. Wang, "Free vibration analysis of a nonlinearly tapered cone beam by adomian decomposition method," *International Journal of Structural Stability and Dynamics*, vol. 18, no. 7, Article ID 1850101, 2018.

[18] Q. Mao and S. Pietrzko, "Free vibration analysis of stepped beams by using Adomian decomposition method," *Applied Mathematics and Computation*, vol. 217, no. 7, pp. 3429–3441, 2010.

[19] F. E. Fakoukakis and F. G. A. Kyriacou, "On the design of a butler matrix-based beamformer introducing low sidelobe level and enhanced beam-pointing accuracy," in *Proceedings of the IEEE-APS Topical Conference on Antennas & Propagation in Wireless Communications*, Torino, Italy, September 2011.

[20] C. Cui, H. Jiang, and Y. H. Li, "Semi-analytical method for calculating vibration characteristics of variable cross-section beam," *Journal of Vibration and Shock*, vol. 31, no. 14, pp. 85–92, 2012.

[21] Q. F Jia, *Mechanical and Structural Vibration*, Tianjin University Press, Tianjin, China, 2007, in Chinese.

[22] H. Liu, *Mechanics of Materials*, Higher Education Press, Beijing, China, 2011, in Chinese, 5th edition.

[23] W. L. Jung and Y. L. Jung, "Free vibration analysis using the transfer-matrix method on a tapered beam," *Computers & Structures*, vol. 164, pp. 75–82, 2016.